

**Controllability of flow turbulence**Shuguang Guan,<sup>1,2</sup> G. W. Wei,<sup>2,3</sup> and C.-H. Lai<sup>4</sup><sup>1</sup>*Temasek Laboratories, National University of Singapore, 5 Sports Drive 2, Singapore 117508, Singapore*<sup>2</sup>*Department of Computational Science, National University of Singapore, Singapore 117543, Singapore*<sup>3</sup>*Department of Mathematics, Michigan State University, East Lansing, Michigan 48824, USA*<sup>4</sup>*Department of Physics, National University of Singapore, Singapore 117542, Singapore*

(Received 11 November 2003; revised manuscript received 6 February 2004; published 16 June 2004)

In this paper, we study the controllability of real-world flow turbulence governed by the two-dimensional Navier-Stokes equations, using strategies developed in chaos control. A case of control/synchronization of turbulent dynamics is observed when only one component of the velocity field vector is unidirectionally coupled to a target state, while the other component is uncoupled. Unlike previous results, it is shown that the dynamics of the whole velocity field cannot be completely controlled/synchronized to the target, even in the limit of long time and strong coupling strength. It is further revealed that the controlled component of the velocity field can be fully controlled/synchronized to the target, but the other component, which is not directly coupled to the target, can only be partially controlled/synchronized to the target. By extending an auxiliary method to distributed dynamic systems, the partial synchronization of two turbulent orbits in the present study can be categorized in the domain of generalized synchronization of spatiotemporal dynamics.

DOI: 10.1103/PhysRevE.69.066214

PACS number(s): 05.45.Gg, 47.27.Rc, 05.45.Xt

**I. INTRODUCTION**

The past decade has witnessed a blossoming in the investigation of chaos control and the synchronization of low-dimensional nonlinear dynamic systems governed by maps or ordinary differential equations (ODEs) [1–5]. Despite the fact that chaos is sensitive to initial conditions, which causes any two neighboring chaotic orbits to diverge exponentially in the state space during time evolution, it is discovered, contrary to our intuition that chaotic dynamics can be generally controlled to a desired periodic target by carefully selected, small perturbations. The target dynamics could be one of the unstable periodic orbits inherently embedded in a strange attractor, or a stationary/periodic orbit, or even another different chaotic orbit. The last situation is conventionally investigated in terms of chaos synchronization. So far, a variety of control strategies, such as the one proposed by Ott, Grebogi, and Yorke [6], time-delay feedback scheme, periodic perturbation, and adaptive scheme, to name just a few, have been successfully applied in achieving chaos control [4]. On the other hand, different scenarios of chaos synchronization, such as complete (identical or exact) synchronization (CS), generalized synchronization (GS), partial synchronization (PS), phase synchronization, and lag synchronization, have been classified and investigated both theoretically and experimentally [3,5]. The synchronization can be regarded as a special means of chaos control. The controllability of low-dimensional systems is well established through the Lyapunov exponent spectrum analysis.

Recently, ideas and strategies originated from the control and synchronization of low-dimensional chaotic systems have been gradually extended to various high-dimensional systems [7], such as the large ensemble of chaotic oscillators described by coupled map lattices and array of chaotic oscillators [8,9], as well as the spatially extended systems naturally described by *discretized* partial differential equations (PDEs) [10–26]. On the one hand, in these distributed sys-

tems, the dimension of the unstable manifold is usually as large as the number of the positive Lyapunov exponents of the system, which in many situations increase linearly with the size of the system. In order to achieve successful control/synchronization of such spatiotemporal chaos, generally the number of controllers (or control signals) needed is of the order of the Lyapunov dimension of the dynamic system. On the other hand, from the practical point of view, it is always desirable to achieve control of the spatiotemporal chaos by using as few controllers as possible. Therefore, the study of the controllability of high-dimensional dynamics is of fundamental importance.

At present, however, little is known about the controllability of infinite dimensional systems, i.e., systems described by nonlinear PDEs. Although earlier numerical examples [10–27] have *indicated* that infinite dimensional (PDE) systems are controllable, in fact, these computational demonstrations are done with the truncation of the original PDE systems because one can only directly deal with finite dimensional systems on a computer. Therefore, the controllability of infinite dimensional systems remains a challenge. A general speculation is that, it is impossible to *fully* control a system with infinite number of positive Lyapunov exponents by using a finite number of controllers. Nevertheless, the abovementioned impossibility does not discourage the effort in exploring practical control of infinite dimensional systems, such as fluid dynamics, governed by the Navier-Stokes equations. After all, all valuable simulations done in computational fluid dynamics are based on truncated systems. The celebrated Lorenz model actually is derived from a model of fluid convection rolls by a dramatical simplification which only retains three modes [28]. The point is that, one should be very careful when drawing a conclusion from computational results.

Flow control is of great scientific significance and economic impact. In fact, what is really required is just a partial control of fluid motion by either passive or active means for

the purpose of drag reduction or for the suppression/enhancement of turbulence. By using an angular momentum injection scheme, it was shown that the vertical component ( $v$ ) of a wake turbulence velocity field could be effectively controlled [29], while the horizontal component ( $u$ ) was left unchecked. Control of two-dimensional (2D) turbulent flow was achieved in our earlier work [16] by using the pinning control strategy developed for chaos control [12–14]. However, in such a study, the control was imposed on both the  $u$  and  $v$  components of the flow field and the number of controllers is compatible with the degree of freedom of the truncated system. In practice, it is both convenient and useful to control a single component of the flow field, such as experimental settings in the lid driven cavity and buoyancy driven cavity [30]. Sometimes, appropriate boundary control could lead to intricate pattern formation in nonlinear PDEs [27].

Chaos control via a single component in a coupled multi-component system is a common practice in the nonlinear dynamics community. For example, in a linearly coupled system of Lorenz oscillators, the controllability can be assessed by eigenvalue analysis. It has been shown that the synchronization of chaos can be achieved by controlling any of the three components [31]. The same idea has been successfully implemented in several cases of chaos control and synchronization in coupled PDE systems [10,11,17,19,21–25]. For example, it has been successfully implemented to control spatiotemporal chaos in laser [10,11] and semiconductor [17,19,21] systems. In both cases the time-delayed feedback control only applies to a variable field that is easily accessible in experiment. In Refs. [22–25], it has also been shown that in certain reaction-diffusion systems, control or synchronization of spatiotemporal chaos can be observed by coupling only one concentration field between the driving and response systems. Remarkably, as demonstrated in Refs. [21,24,25], the whole spatiotemporal dynamics can even be successfully controlled by adding perturbation of scalar time series to only one degree of freedom of the spatially extended system.

Therefore, it is interesting to examine the controllability of turbulent flow governed by Navier-Stokes equations via the single component control and using the pinning control strategy originated from chaos control. Our interest of controlling real-world turbulence from the perspective of chaos control is motivated by the following facts. It is well known that real-world turbulence represents the most complicated spatiotemporal dynamics. Till now, the control of flow turbulence remains a challenging task in many scientific and engineering fields [32]. It is believed that turbulence control could benefit from the lessons in chaos control, which has been intensively studied in the last decade. With so many aforementioned successful examples in chaos control, one might take it for granted that by applying the pinning control only to either  $u$  or  $v$  component of the flow velocity field, the whole velocity field  $(u, v)$  could be completely controlled to the target, i.e., a spatially periodic and temporally varying velocity field, or another turbulent orbit in our study. However, the findings in the present work indicate that this is not the case for the dynamic system of flow turbulence. Unlike the previous findings [17,22,23], it is found that the whole velocity field  $(u, v)$  can only be partially controlled to the

desired targets in the sense that the control error is bounded by a small constant, but not zero. This situation does not improve with the increase of the coupling strength. Further analysis reveals that the  $u$  component, which is directly coupled to the control signals, actually can be completely controlled to the target, whereas, the  $v$  component fails to do so, though it is coupled to  $u$  via the Navier-Stokes equations. In the framework of synchronization, it is shown that this phenomenon further can be characterized in terms of generalized synchronization by using the response-auxiliary system method. Therefore, our work shows that GS (as compared to complete synchronization) can also be observed between two identical coupled PDE systems when the coupling between them is insufficient. It is believed that the present findings not only enhance our understanding of control/synchronization in distributed systems, but also shed light on the real-world turbulence control.

This paper is organized as follows. In the following section, the dynamic model and numerical method are briefly described. In Sec. III, the control of flow turbulence to a spatially periodic pattern, and the synchronization between two different turbulent orbits by using unidirectional pinning coupling, are considered. The results are presented there. Moreover, the relation between the present case and partial synchronization, as well as the generalized synchronization, is discussed in Sec. IV. A conclusion ends the paper.

## II. THE MODEL AND NUMERICAL METHOD

For simplicity, in the present study we investigate the control of flow turbulence described by the two-dimensional Navier-Stokes equations. The dynamics of two-dimensional turbulence, which exhibits many interesting features, differs fundamentally from its three-dimensional counterpart [33]. Its research is of importance to the understanding of geophysics, meteorology as well as magnetohydrodynamics. In the framework of direct numerical simulation, we consider the two-dimensional Navier-Stokes equations,

$$u_t + uu_x + vu_y = -p_x + \frac{1}{\text{Re}}(u_{xx} + u_{yy}), \quad (1)$$

$$v_t + uv_x + vv_y = -p_y + \frac{1}{\text{Re}}(v_{xx} + v_{yy}), \quad (2)$$

with the incompressible condition acting on the whole flow field

$$u_x + v_y = 0, \quad (3)$$

where  $(u, v)$  is the two-dimensional velocity vector field,  $p$  the pressure,  $\text{Re}$  the Reynolds number, and the subscripts denote the derivatives. The flow is bounded in a square domain  $[0, 2\pi] \times [0, 2\pi]$  with doubly periodic boundary conditions. To solve the incompressible Navier-Stokes equations within the turbulence regime, the choice of an appropriate numerical scheme is particularly important due to the lack of a governing equation for the pressure field, while the velocity fields are over determined. In the present work, the spatial and temporal discretization are carried out by applying Fou-

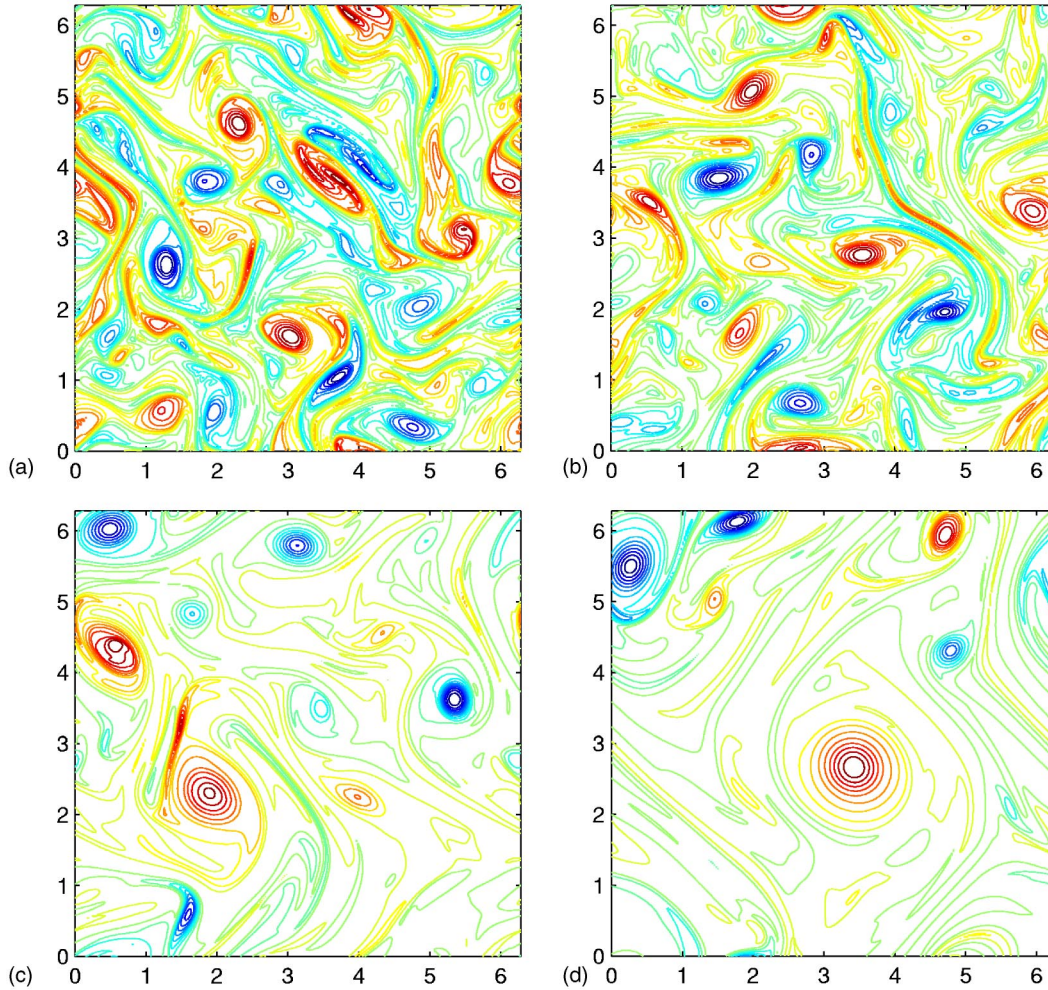


FIG. 1. The flow turbulence to be controlled (the response system). Contour plots showing the evolution of the vorticity field ( $\omega = v_x - u_y$ ) at (a)  $t=5$ , (b)  $t=10$ , (c)  $t=30$ , (d)  $t=50$ , respectively. The initial energy and the enstrophy are 0.10 and 2.50, respectively.

rier pseudospectral method and the Adams-Bashforth-Crank-Nicolson scheme, respectively. The above numerical scheme ensures divergence-free velocity fields and has the spectral precision for spatial discretization and second order precision for time integration. Its validity has been extensively tested [16,34,35].

It is shown that the dynamics of freely decaying two-dimensional turbulence depends on the initial conditions. Usually the initial conditions are given in Fourier (wave number) space such that the initial energy spectrum satisfies certain desired form [36]. Two commonly used initial energy spectral profiles are

$$E(k,0) \sim k e^{-(k/k_0)^2}, \quad (4)$$

$$E(k,0) \sim k^4 e^{-(k/k_0)^2}. \quad (5)$$

Here the constant  $k_0$  is an adjustable constant for the wave number at which the energy spectrum peaks.

The parameter settings in the current simulation are as follows. The dynamics of Eqs. (1)–(3) is set at the turbulent regime by taking  $\text{Re}=5000$ . For the response system, i.e., the fluid system to be controlled, the initial conditions are taken

to satisfy Eq. (4) with  $k_0=5.0$ . The time increment  $\Delta t$  is chosen to be 0.0025 and  $256 \times 256$  grid points are used ( $N_x=N_y=256$ ). The total integration length is 50, which covers several hundreds of initial eddy turnover time. The typical dynamic characteristics of two-dimensional turbulence, such as the formation, interaction, and evolution of coherent vortices, are shown in Fig. 1. Here, following the convention, the turbulence field is visualized in terms of vorticity contours. All the numerical results have been confirmed by using different grids and time increments.

### III. CONTROL OF TURBULENCE

The viability and effectiveness of controlling flow turbulence by using chaos control strategies, such as global pinning and local pinning, have been studied recently [16]. In the present work, we further show that the turbulent dynamics governed by the Navier-Stokes equations can be partially controlled to certain spatially periodic target by only coupling one velocity component  $u$ , i.e., the  $x$  component of the velocity field, to the counterpart of the target. This is motivated by the fact that in experiments controlling one compo-

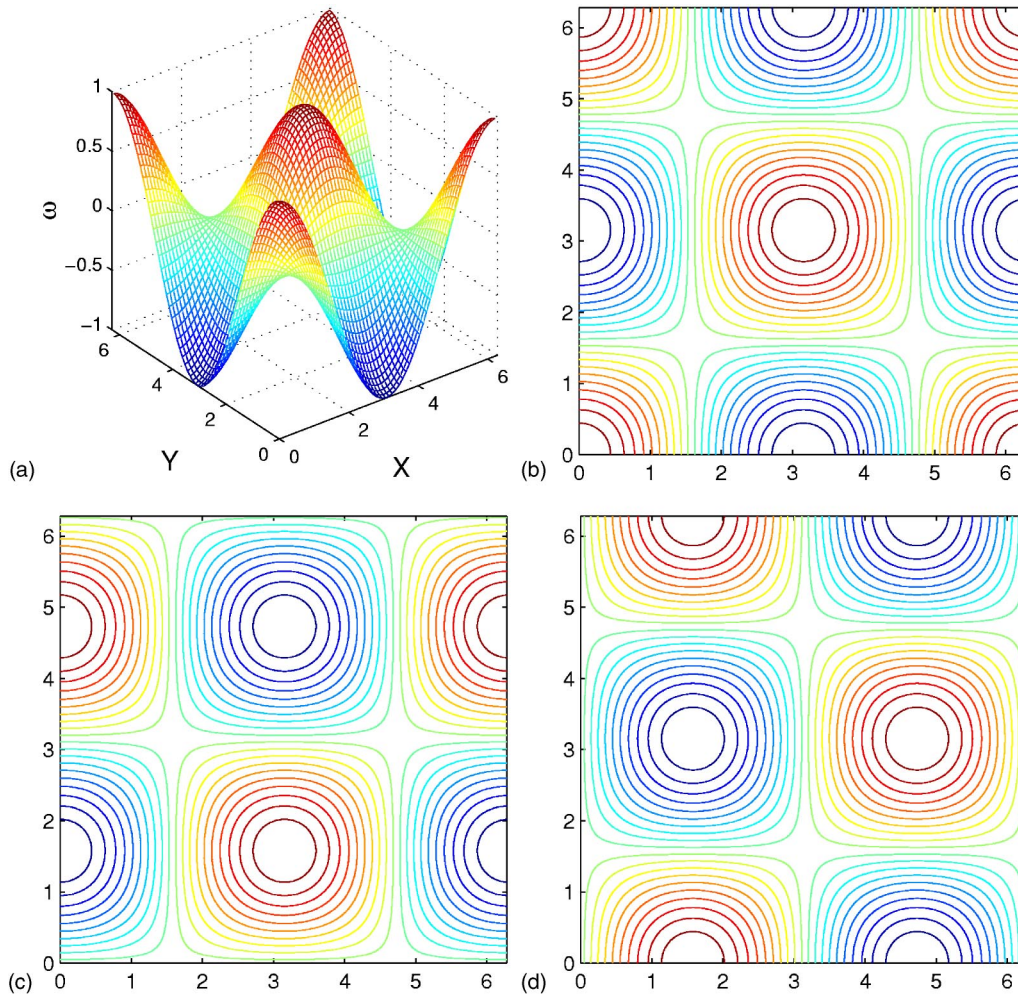


FIG. 2. The spatially periodic target. (a) the vorticity mesh, (b) the vorticity contour, (c) the contour of  $u$ , (d) the contour of  $v$ .

ment of the velocity field could be easier than controlling the whole velocity field. To this end, we apply the pinning control, which is a basic and commonly used strategy in the control of spatiotemporal chaos,

$$f(u, u_T) = -\epsilon(u - u_T), \quad (6)$$

to the right-hand side of Eq. (1), with  $u_T$  being the corresponding  $x$  component of the velocity field of the target, and  $\epsilon > 0$  the coupling strength. It is notable that in this control scheme, the perturbations or the control signals, are only added to the  $x$  component of the velocity field. The divergence-free condition Eq. (3) is effectively maintained under the present perturbation. One may reasonably think that the whole velocity field could be changed by this perturbation, but to what extent it converges to the target is yet to be ascertained.

### A. Periodic target

The target we considered is a spatially periodic and temporally varying analytical solution of the Navier-Stokes equations [34]

$$u_T(x, y, t) = -\gamma \cos(kx) \sin(ky) e^{-2k^2 t / \text{Re}},$$

$$v_T(x, y, t) = \gamma \sin(kx) \cos(ky) e^{-2k^2 t / \text{Re}}, \quad (7)$$

where  $k$  is the wave number taking an integer value ( $k=1$  in the present study), and  $\gamma$  is a constant which is chosen as 0.05 in this study. In Fig. 2, the mesh and contour plot of the target is shown. For  $t < 5$ , the response system Eqs. (1)–(3) freely evolves without any control. This ensures that the system passes the transient stage and enters the turbulent regime. The coupling term Eq. (6) then is switched on at the right-hand side of Eq. (1), denoting the control of the  $x$ -component of the velocity field.

The asymptotic behavior of the response system with control has been studied with respect to the coupling strength  $\epsilon$ . The parameter studied in the present work ranges from  $\epsilon = 0.01$  to  $\epsilon = 10$ . It is found that with small coupling strength, roughly  $\epsilon < 0.05$ , the weak control cannot convert the turbulent dynamics to the periodic target. Nevertheless, this very small perturbation acting as a driving force can direct the dynamics to another turbulent orbit. For instance, Fig. 3(a) shows a turbulent state under small control, which is totally different from Fig. 1(d), the state without any control. When  $\epsilon \geq 0.05$ , it is observed that the dynamics of the response system can be partially controlled to the target. Figure 3

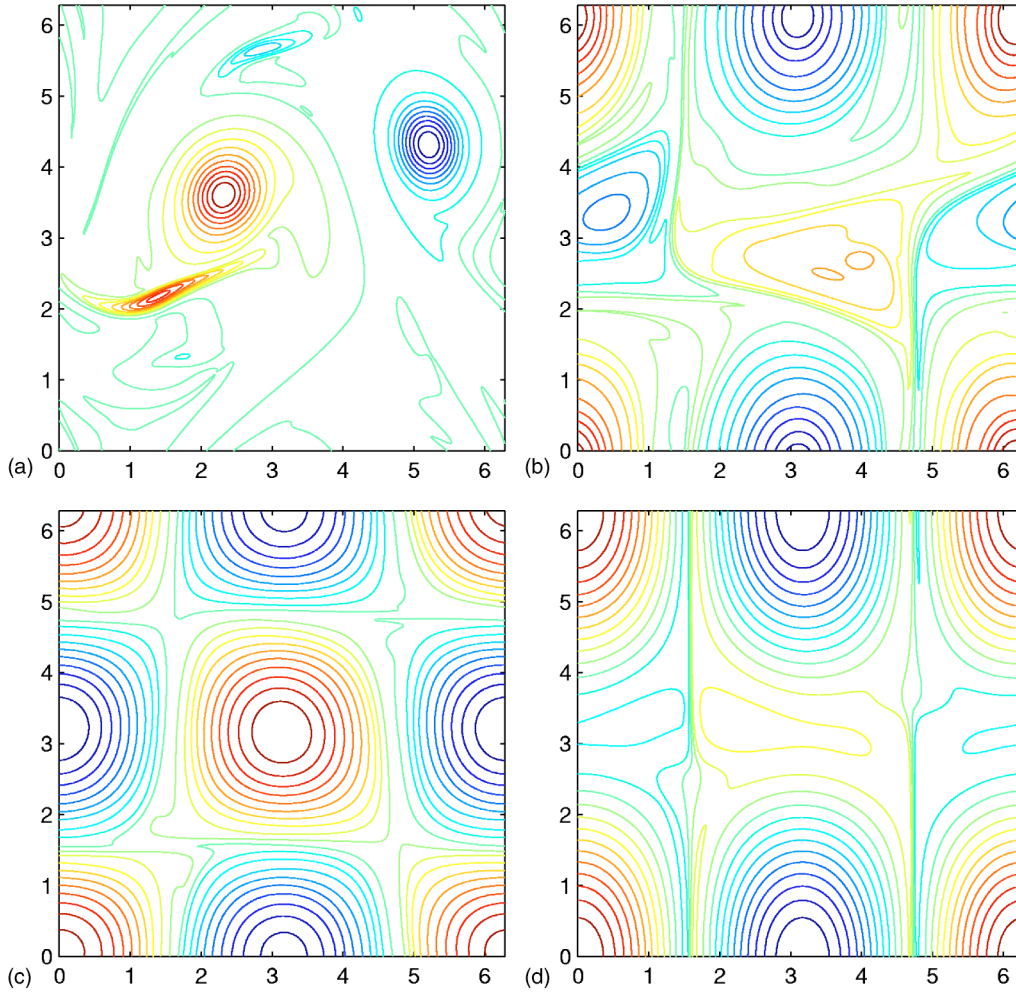


FIG. 3. The partial control of turbulence. The contour plots of the vorticity field of the response system with control at  $t=50$ . (a)  $\epsilon=0.01$ , (b)  $\epsilon=0.05$ , (c)  $\epsilon=0.1$ , (d)  $\epsilon=0.5$ .

shows that the turbulence in the response system can partially converge to the spatially periodic target when the coupling strength is strong enough.

In order to characterize this partial control of the turbulence, we define the control error between two vorticity fields at a specific time as

$$\sigma_{\omega}(t) = \left\{ \frac{1}{N_x N_y} \sum_{i=1, j=1}^{N_x, N_y} [\Delta\omega(i, j, t)]^2 \right\}^{1/2}, \quad (8)$$

where  $\Delta\omega(x, y, t) = \omega(x, y, t) - \omega_T(x, y, t)$ , and  $i, j$  are the grid indices. In the case of complete control, we should have

$$\lim_{t \rightarrow \infty} \sigma_{\omega}(t) \rightarrow 0. \quad (9)$$

Figure 4(a) characterizes the partial turbulence control in terms of the control error defined above. If we compare Figs. 3 and 4(a) with the results of the pinning control of the whole vector field ( $u, v$ ) in Ref. [16], immediately we can identify several differences. First of all, it is clearly shown that in the present case the dynamics of the response system cannot be completely controlled to the target. Instead, it

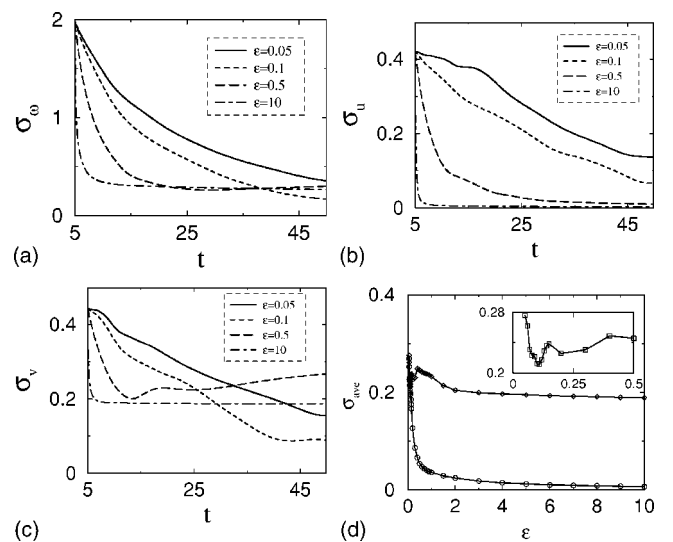


FIG. 4. Characterizing the control of turbulence to a spatially periodic target. The control error vs time for (a) the vorticity, (b)  $u$ , and (c)  $v$ . (d) The time-averaged control error for  $u$  (the circle) and  $v$  (the diamond), respectively.

could only be partially controlled to the target if the coupling strength is strong enough. By partial control, we mean that the control error between the response and the target system is bounded by a small but nonzero number. However, the control error does not decrease monotonically with the increase of the coupling strength. There exists a moderately large coupling strength, approximately around  $\epsilon=0.1$ , which turns out to be the optimal value for the control. For instance, although initially, the control error at  $\epsilon=0.1$  decays slower than that when  $\epsilon>0.1$ , in a later time, its value can be smaller than that when  $\epsilon>0.1$  as shown in Fig. 4(a). The vorticity contours in Fig. 3 further confirms that at  $\epsilon=0.1$  the controlled vorticity Fig. 3(c) closely resembles the target Fig. 2(b), showing the best control effect among all the coupling strengths. Second, by regression analysis, it is found that the control error which characterizes the convergence between two dynamic orbits no longer decays exponentially with respect to time. Finally, in the limit of  $\epsilon$  approaching the infinity, the control error approaches a small nonzero constant, instead of zero in the case of complete control [16], i.e.,

$$\lim_{t \rightarrow \infty, \epsilon \rightarrow \infty} \sigma_\omega(t) \rightarrow c, \quad (10)$$

with  $c \approx 0.24$  here. It should be pointed out that the existence of an optimal control strength has already been found in reaction-diffusion system employing time-delay feedback [17,19,21], where generally the successful control only occurs between a lower and an upper limit of the control strength. Nevertheless, there are some differences between these findings and the current result. In Refs. [17,19,21], the target states can be completely stabilized. The optimal control is achieved when the control signal vanishes and the largest Lyapunov exponent reaches its minimum. In our case, the complete convergence to the target state is impossible, only partial control can be obtained. The optimal control here refers to the best convergence to the target. Furthermore, the control scheme in the present study is different from that in Refs. [17,19,21].

The feature of the present control deserves further analysis. Since in the present study only the  $x$  component of the velocity field is directly under control, naturally we would like to check the control efficiency of the  $u$  and  $v$  fields separately. This can be done by analyzing the control error between the corresponding components between the target and the response system. Specifically, we compute the control error  $\sigma_u$  and  $\sigma_v$  by replacing  $\Delta\omega$  in Eq. (8) with  $\Delta u = u(x, y, t) - u_T(x, y, t)$  and  $\Delta v = v(x, y, t) - v_T(x, y, t)$ , respectively. The control errors versus time with different coupling strength are shown in Figs. 4(b) and 4(c). We found that for the  $x$  component  $u$ , the control error decreases monotonically with the increase of the coupling strength. In the limit of strong coupling strength, the control error approaches zero. Moreover, for a given coupling strength, the control error reaches zero as long as  $t$  is large enough. Although the total velocity field  $(u, v)$  cannot be completely control to the target as shown in Fig. 3, Fig. 4(b) reveals that the  $x$  component  $u$ , which is directly coupled to the target, actually converges completely to the target. This complete convergence can be further confirmed in Fig. 5, where the evolution of the field  $u$

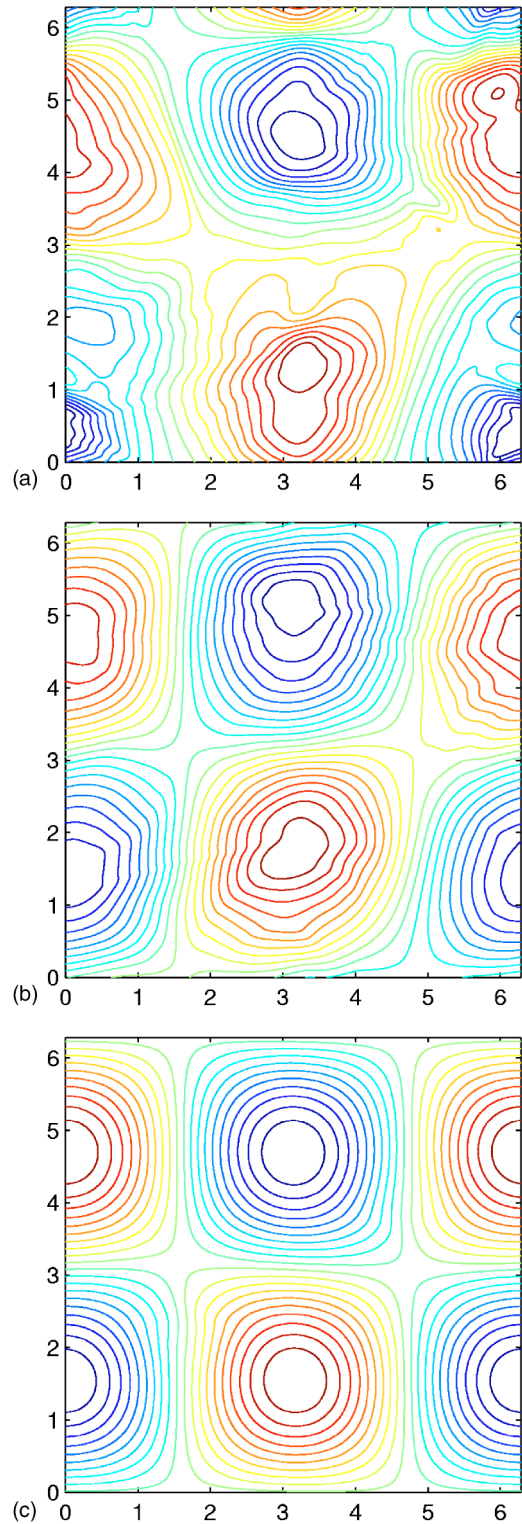


FIG. 5. Contour plots of  $u$  at  $t=50$  for different coupling strength. (a)  $\epsilon=0.05$ . (b)  $\epsilon=0.1$ . (c)  $\epsilon=0.5$ . Compared with the target Fig. 2(c), the complete convergence of  $u$  to the target can be achieved when the coupling strength is large enough.

has been plotted for certain typical coupling strength, indicating the full convergence of the  $x$  component  $u$  to the target [shown in Fig. 2(c)] when the coupling strength is large enough.

On the other hand, however, as shown in Fig. 4(c), the control of the  $y$  component  $v$  turns out to be a different scenario. The control error does not decrease monotonically with the increase of the coupling strength. There is an optimal coupling strength at which the component  $v$  is most efficiently controlled to the target. When the coupling strength is further increased to a large enough value, the control error finally approaches a nonzero small constant. Therefore, for the  $y$  component  $v$ , it can only be partially controlled to the target. Figure 6 shows the partial control of the  $y$  component  $v$  to the target shown in Fig. 2(d). The above dynamic features of the partial control of turbulence can be better demonstrated in Fig. 4(d), where the time-averaged control errors versus the coupling strength for both  $u$  and  $v$  are plotted. Clearly it is illustrated that the time-averaged control error of  $u$  decreases monotonically to zero with the increase of the coupling strength. Notably, the time-averaged control error of  $v$  oscillates in the interval  $[0.01, 0.5]$ , reaches the minimum at about  $\epsilon=0.1$ , and gradually approaches a constant when  $\epsilon>0.5$ . Based on the above analysis, we conclude that in the present flow system, by applying control to only one component of the vector field, the dynamics of the response system cannot be fully controlled to the target, even in the regime of strong coupling. This finding is fundamentally different from previous ones [10,11,17,19,21–25]. Moreover, it is also different from the study in Ref. [16], where the pinning control is applied to the whole velocity field. An example comparing these two control strategies is shown in Fig. 7.

### B. Turbulent target

Next, we control the turbulent dynamics of the response system into another turbulent orbit. In fact, the control of chaos using unidirectional coupling is equivalent with the synchronization between the dynamics of two systems [37]. When the target is chaotic, chaos control is more natural to be understood in terms of synchronization. We follow this convention to describe this second example in the framework of synchronization. The turbulent target is also generated from Eqs. (1)–(3), but the initial conditions satisfy Eq. (5) with  $k_0=3.0$ . Figure 8 shows the evolution of the vorticity of this target. It is different from the turbulence of the response system as shown in Fig. 2. Similarly, only the  $x$  component  $u$  of the velocity field in the response system is unidirectionally driven by the target system through coupling term Eq. (6).

Once again, it is found that the turbulent dynamics of the response system can only be partially synchronized with the target. Figure 9 characterizes this partial synchronization in terms of the synchronization error defined in Eq. (8). In Fig. 9(a), it is shown that when the coupling strength is large enough, the synchronization error of the vorticity between two systems becomes bounded and decreases with time. However, even in the strong limit of the coupling strength, this synchronization error cannot approach zero; instead it approaches a small nonzero constant. Similar to the first example, Figs. 9(b) and 9(c) reveal that the  $x$  component  $u$  does fully synchronize with the target, while the component  $v$  fails to do so. This accounts for the partial synchronization of

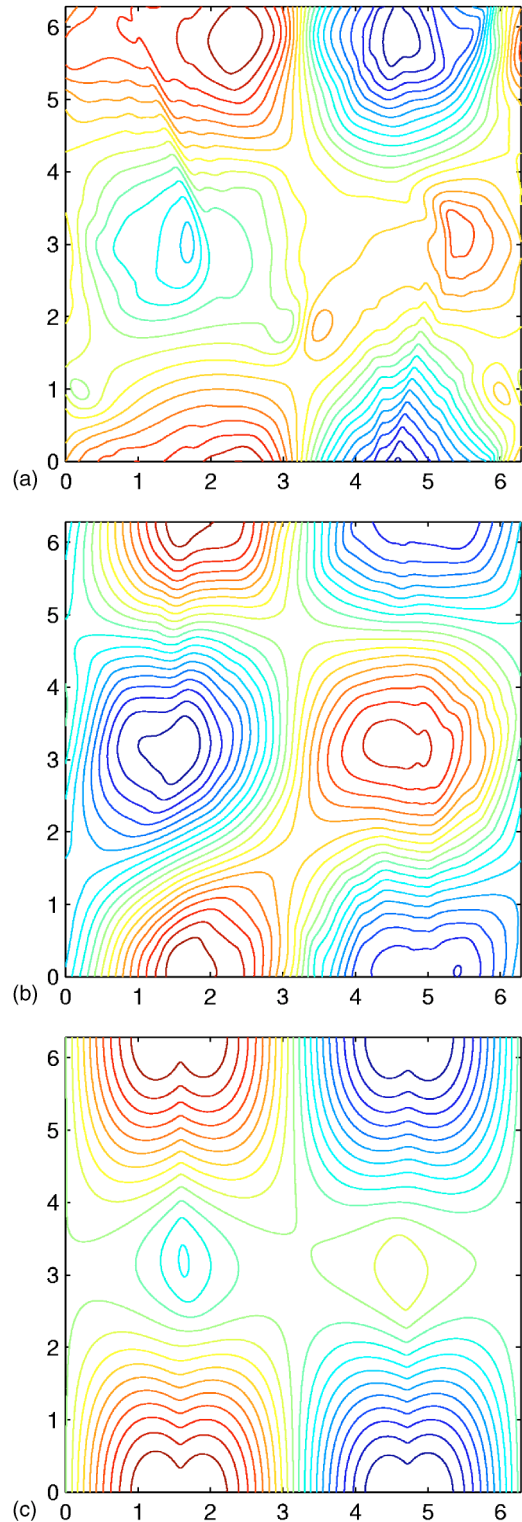


FIG. 6. Contour plots of  $v$  at  $t=50$  for different coupling strength. (a)  $\epsilon=0.05$ . (b)  $\epsilon=0.1$ . (c)  $\epsilon=0.5$ . Compared with the target Fig. 2(d),  $v$  only partially converges to the target.

the whole velocity vectors between the response and target systems. In addition, comparing Fig. 9 with Fig. 4, we found that generally a stronger coupling strength is needed to synchronize the dynamics of the response system with the turbulent target than the spatially periodic one. We have care-

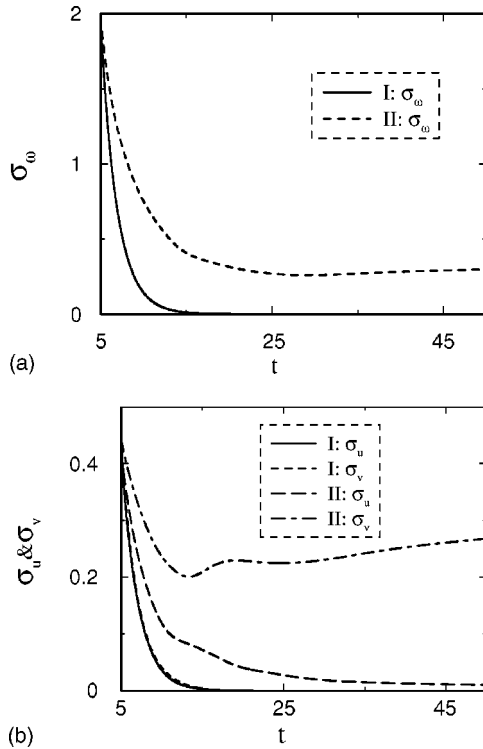


FIG. 7. Comparison the effectiveness of two different control strategies. One is to control both  $u$  and  $v$  (I), the other is only control  $u$  (II).  $\epsilon=0.5$  in both cases. (a) The control errors of vorticity. (b) The control errors of  $u$  and  $v$ . The solid line and the dashed line coincide.

fully examined the evolution of the  $u$  field and found that in this case only when  $\epsilon > 0.5$  can the component  $u$  be regarded as synchronized with the target in a practical sense. This is confirmed in Figs. 9(b) and 9(c), where the synchronization error of  $u$  decreases to nearly zero and the synchronization error of  $v$  becomes bounded, approaching a small constant when  $\epsilon > 0.5$ . Thus the critical coupling strength in the case of turbulent target is roughly one order larger than that in the case of a spatially periodic target. In this sense, it is more difficult to control the system into a turbulent target than into a spatially periodic one. Another important point illustrated by Fig. 9(c), compared with Fig. 4(c), is that the synchronization error approaches a smaller constant, roughly 0.065 in the second example. This implies that in the limit of long time and strong coupling strength, the dynamics of two  $v$  fields can be more “correlated” than in the case of spatially periodic target. In other words, the two turbulent orbits can move “closer” than between a turbulent orbit and a spatially periodic target as in our first example. This feature is further manifested in Fig. 9(d), where the time-averaged control/synchronization errors versus the coupling strength for the two different targets are plotted for a comparison. Clearly, in both cases, the control/synchronization errors of the  $u$  field approach zero with the increase of the coupling strength, showing the full convergence of the  $u$  fields between the target and the response system. But for the  $v$  field, the control/synchronization errors approach small nonzero constants in the strong coupling limit, showing the  $v$  field can

only be partially converged to the target. Note that in our control configuration, the  $v$  field does not directly couple to the target. Our results thus imply that there exist certain dynamic systems (such as fluid systems) in which complete control of the dynamics cannot be achieved by controlling only part of its state variables. It is reported recently that a pair of fully resolved quasi-2D fluid models will synchronize only when the small-scale/high-frequency components of the flow are coupled [38]. In other words, only when all the active degrees of freedom in such a fluid system are coupled, can the fluid dynamics be completely synchronized. This result is consistent with our findings in the present study.

#### IV. DISCUSSION OF THE RESULTS

In the framework of chaos synchronization, it is interesting to compare the present findings with the existing synchronization scenarios, especially the PS and the GS, in chaotic systems. The PS refers to the situation between two dynamic systems where some state variables are completely (or in practical sense) synchronized, but others (at least one) are not [39,40]. According to this definition, the phenomenon found in this study apparently belongs to this category. It should be pointed out that in the literature, the terminology PS sometimes also refers to the clustering phenomenon occurring in large ensembles of coupled chaotic oscillators [41–43]. The present results are not relevant to this situation.

The GS is another well known synchronization phenomenon in chaotic systems, in which the dynamics of the drive and the response system does not coincide; instead they are asymptotically related [44]. The question naturally arises is: what is the relation between PS and GS? Since so far there are no strict mathematical definitions for these concepts, we can only understand the relation between them qualitatively. Conceptually, these two concepts overlap somewhat. In certain cases of PS, if the unsynchronized state variables are totally uncorrelated (generally this is hard to detect, but sometimes it can be characterized by Lyapunov exponents as in Ref. [39]), the two systems would be regarded as pure PS, but not GS. In other cases of PS, if there exists certain functional relation between the unsynchronized state variables of two systems, this PS could also belong to the case of GS. One effective way to detect GS in low-dimensional chaos synchronization is the auxiliary system method [45], in which a replica of the response system, but with different initial condition, is simultaneously driven by the same driving system. Therefore, the usual complicated functional relation between the dynamics in the driving and response systems, i.e., the GS, can be effectively detected in the state space of response and auxiliary systems as complete synchronization. In the present study, we extend this method to detect the GS between spatially extended systems. Due to the nature of extremely high dimensions in the present study, it is impossible to check the dynamics in all the spatial sites between the response and auxiliary systems as in Ref. [46]. However, certain space-averaged global quantities, such as the global synchronization error defined in Eq. (8) can be conveniently used to detect GS. If the spatiotemporal dynamics between the driving and response systems achieves GS,

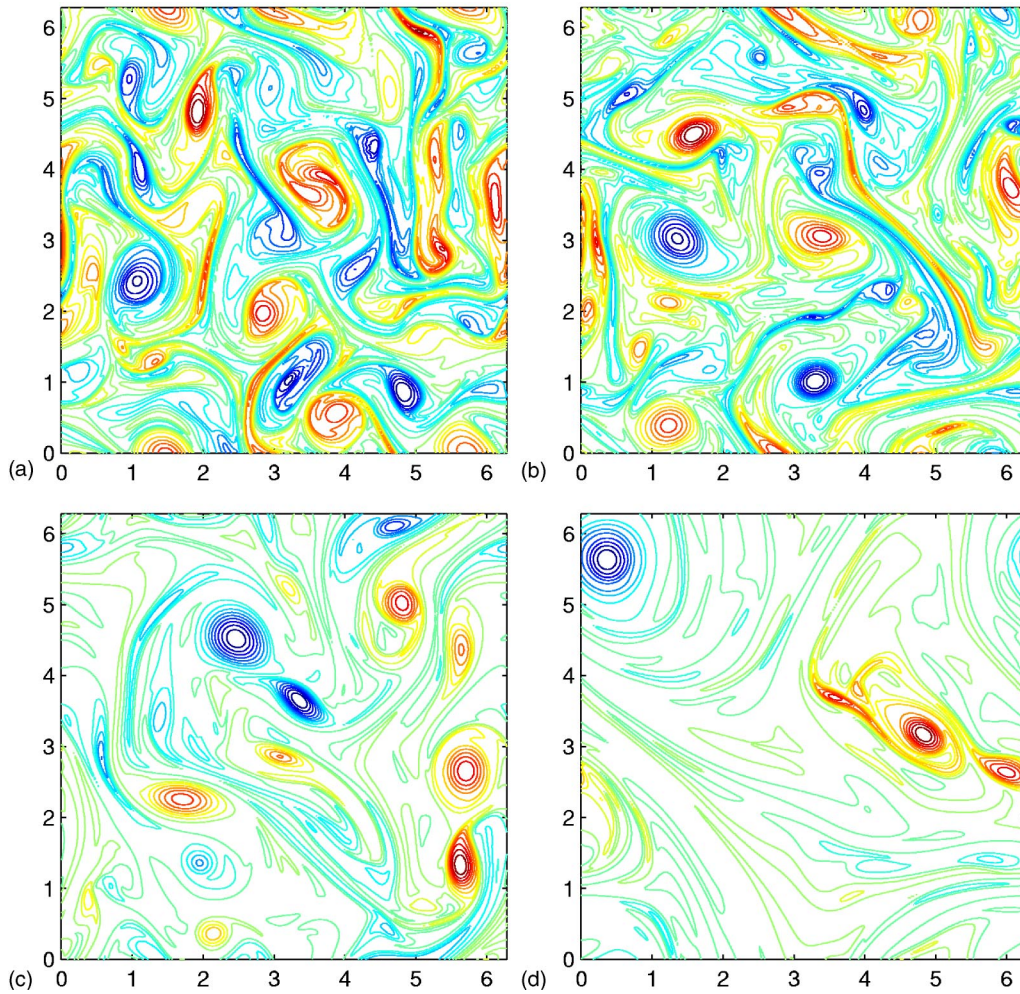


FIG. 8. The flow turbulence in the drive system. Contour plots showing the evolution of the vorticity field at (a)  $t=5$ , (b)  $t=10$ , (c)  $t=30$ , (d)  $t=50$ , respectively. The initial energy and the enstrophy are 0.10 and 2.31, respectively.

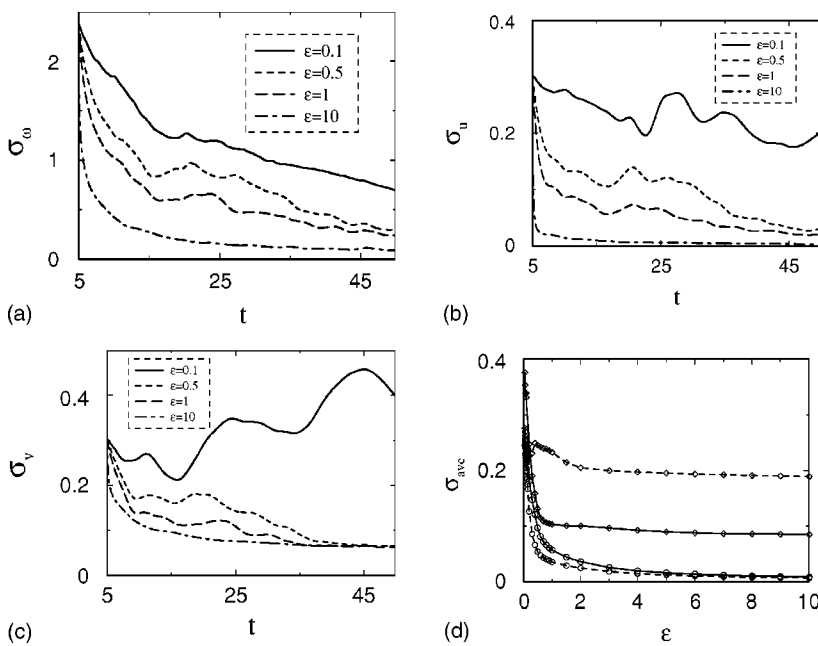


FIG. 9. Characterizing the synchronization of two turbulent orbits. The synchronization error vs time for (a) the vorticity, (b)  $u$ , and (c)  $v$ . (d) The time-averaged synchronization error for  $u$  (the circle), and  $v$  (the diamond), respectively. The time-averaged control errors in the first case are also plotted in dotted lines for comparison.

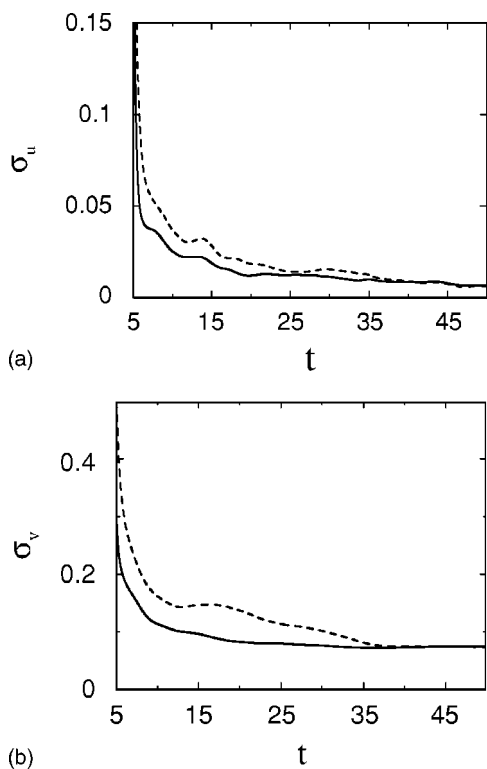


FIG. 10. Detecting the GS between two turbulent orbits. The synchronization errors of (a)  $u$  and (b)  $v$ . The solid lines, the synchronization error between the drive and the response system; the dashed lines, the synchronization error between the drive and the auxiliary system.

asymptotically the global synchronization errors between the driver and the response, which is a time series, will gradually converge to that between the driving and auxiliary systems. Therefore, the global synchronization error between the response and auxiliary systems will approach zero after long time evolution. We used this method to check whether the partial synchronization in this study is GS or not. The results are shown in Fig. 10, where the global synchronization errors between the response and auxiliary systems clearly show the trend towards zero when time approaches infinity. Therefore, the present synchronization phenomenon can also be understood in terms of GS.

It is well known that for the coupled nonidentical dynamic systems, either parametrically different or physically different, GS is generally expected to be observed, but CS is forbidden. On the other hand, for the coupled identical dynamic systems, CS is the usual outcome. Recently in Refs. [47,48], it is shown that GS can also take place in two coupled identical ODE systems before the coupling becomes strong enough to achieve CS. Our findings in the present work further demonstrate that the GS could also occur between two unidirectionally coupled identical PDE systems. It should be pointed out that the GS in Refs. [47,48] happens when the coupling is weak. However, in the current case, the GS can take place even in strong coupling strength, but the coupling itself is not sufficient in the sense that only one component of the vector field is directly linked to the target. As a result, even the strong coupling strength fails to achieve

the full synchronization between two flow systems. It turns out that flow systems are more difficult to control in the above sense.

For infinite dimensional dynamic systems, it is desirable to use as less as possible controllers to achieve the complete control. This is of great importance from the point of view of control efficiency in practice. To this end, one method is to reduce the number of local controllers, as demonstrated in Refs. [12–14,16]. Another method is to control a single component in the multiple-component dynamic systems, which is commonly used in controlling low-dimensional systems as well as high-dimensional systems [10,11,17,19,21–25]. In the present paper, using pinning feedback strategy, we show that full control of flow turbulence cannot be achieved by the second method, while it is successful in the first method [16]. This finding implies that although the above two methods are both designed to reduce the dimensionality of the control signals, the results might be essentially different.

In the present work, we only focus on the pinning feedback control strategy for the controlling of flow turbulence. It should be pointed out that there are other prevalent techniques which have been successfully developed in taming spatiotemporal chaos, for example, the time-delay feedback [10,11,17–21,24,25] and the forcing or entrainment [9,24,26]. These methods have some advantages, such as no predesigned target needed and easily implemented in experiment. For the time-delay feedback strategy, it usually works well in the dynamic systems which have an inherent characteristic time scale so that the delay time can be appropriately determined. For example, in many reaction-diffusion systems, there exist unstable traveling wave solutions in the regime of spatiotemporal chaos. However, the coupling of hydrodynamic modes in turbulence is quite complicated (usually studied in Fourier space) and is fundamentally different from the reaction-diffusion systems. Generally there is no such a characteristic time scale for flow turbulence. Therefore, it is difficult to apply the time-delay feedback control method to flow systems. In our numerical experiments, we have also tried the forcing strategy in order to suppress turbulence. We considered two situations. In one case, a temporally sinusoidal perturbation is globally added to the flow field; in the other case, the feedback perturbation is chosen as proportional to the square of the velocity field. In the first case, we observe that generally the perturbation drives the flow system to be unstable. This is understandable since such homogeneous perturbation has every Fourier mode, thus drives the flow at each scale. In the second case, the forcing does change the turbulent field, but seems difficult to tame the turbulence, sometimes even enhances it. In fact, turbulence usually can be enhanced and sustained by suitable local forcing in Fourier space [49]. How to choose appropriate forcing form so that flow turbulence can be suppressed or tamed deserves further systematic investigation and will be addressed elsewhere.

### V. CONCLUSION AND DISCUSSION

In the present work, the controllability of real-world flow turbulence has been theoretically investigated by employing

the strategies developed in the domain of chaos control. The purpose of the work is to reexamine the validity of some chaos control techniques that have been shown to be successful in low and moderately high-dimensional systems for turbulence control. One of these techniques is to control flow turbulence by coupling only one component of the velocity field in the Navier-Stokes equations to a target dynamics, which can be a spatially periodic and temporally varying analytical solution of the Navier-Stokes equations, or a turbulent orbit that is different from the response system. It is hoped that this technique might lead to practical application to flow control since in reality it is often more convenient to control fluid flows by a selected velocity component. Contrary to previous findings [10,11,17,19,21–25], it is found that the whole velocity field ( $u, v$ ) cannot be completely controlled/synchronized to the target through the pinning control of one component of the vector field, even in the limit of long control time and strong coupling strength. The control was characterized in terms of control error versus

time and the time-averaged control error versus the coupling strength. Since the control error approaches a small nonzero constant, the present phenomenon can be regarded as a partial control/synchronization. Further analysis reveals that the controlled component of the velocity, i.e., the  $u$  field, actually can be fully controlled/synchronized to the target, but the component  $v$ , which does not directly couple to the target, can only be partially controlled/synchronized. Therefore, the present finding provides an example of controllability of flow turbulence which demonstrates different characteristics from many other distributed dynamic systems and extends our knowledge in this research direction.

#### ACKNOWLEDGMENTS

This work was supported by the National University of Singapore, the Temasek Laboratories at National University of Singapore, and Michigan State University.

- 
- [1] T. Kapitaniak, in *Controlling Chaos: Theoretical and Practical Methods in Nonlinear Dynamics* (Academic, London, 1996), and references therein.
- [2] G. Chen and X. Dong, in *From Chaos to Order: Methodologies, Perspectives and Applications* (World Scientific, Singapore, 1998).
- [3] A. Pikovsky, M. Rosenblum, and J. Kurths, in *Synchronization: A Universal Concept in Nonlinear Science* (Cambridge University Press, Cambridge, 2001).
- [4] S. Boccaletti, C. Grebogi, Y.-C. Lai, H. Mancini, and D. Maza, *Phys. Rep.* **329**, 103 (2000).
- [5] S. Boccaletti, J. Kurths, G. Osipov, D. L. Valladares, and C. S. Zhou, *Phys. Rep.* **366**, 1 (2002).
- [6] E. Ott, C. Grebogi, and J. Yorke, *Phys. Rev. Lett.* **64**, 1196 (1990).
- [7] M. Ding, E. Ding, W. L. Ditto, B. Gluckman, V. In, J.-H. Peng, M. L. Spano, and W. Yang, *Chaos* **7**, 644 (1997).
- [8] G. W. Wei, M. Zhan, and C.-H. Lai, *Phys. Rev. Lett.* **89**, 284103 (2002).
- [9] G. Baier, S. Sahle, J.-P. Chen, and A. A. Hoff, *J. Chem. Phys.* **110**, 3251 (1999).
- [10] M. E. Bleich, D. Hochheiser, J. V. Moloney, and J. E. S. Socolar, *Phys. Rev. E* **55**, 2119 (1997).
- [11] D. Hochheiser, J. V. Moloney, and J. Lega, *Phys. Rev. A* **55**, R4011 (1997).
- [12] J. Xiao, G. Hu, J. Yang, and J. Gao, *Phys. Rev. Lett.* **81**, 5552 (1998).
- [13] S. Boccaletti, J. Bragard, and F. T. Arecchi, *Phys. Rev. E* **59**, 6574 (1999).
- [14] L. Junge and U. Parlitz, *Phys. Rev. E* **61**, 3736 (2000).
- [15] G. W. Wei, *Phys. Rev. Lett.* **86**, 3542 (2001).
- [16] S. Guan, Y. C. Zhou, G. W. Wei, and C.-H. Lai, *Chaos* **13**, 64 (2003).
- [17] G. Franceschini, S. Bose, and E. Schöll, *Phys. Rev. E* **60**, 5426 (1999).
- [18] N. Baba, A. Amann, E. Schöll, and W. Just, *Phys. Rev. Lett.* **89**, 074101 (2002).
- [19] O. Beck, A. Amann, E. Schöll, J. E. Socolar, and W. Just, *Phys. Rev. E* **66**, 016213 (2002).
- [20] W. Just, S. Popovich, A. Amann, N. Baba, and E. Schöll, *Phys. Rev. E* **67**, 026222 (2003).
- [21] J. Unkelbach, A. Amann, W. Just, and E. Schöll, *Phys. Rev. E* **68**, 026204 (2003).
- [22] L. Kocarev, Z. Tasev, and U. Parlitz, *Phys. Rev. Lett.* **79**, 51 (1997).
- [23] P. Parmananda, *Phys. Rev. E* **56**, 1595 (1997).
- [24] P. Parmananda and M. Eiswirth, *J. Phys. Chem. A* **103**, 5510 (1999).
- [25] P. Parmananda and J. L. Hudson, *Phys. Rev. E* **64**, 037201 (2001).
- [26] P. Parmananda, B. J. Green, and J. L. Hudson, *Phys. Rev. E* **65**, 035202(R) (2002).
- [27] S. Guan, C.-H. Lai, and G. W. Wei, *Physica D* **151**, 83 (2001); **163**, 49 (2002); **176**, 19 (2003).
- [28] E. N. Lorenz, *J. Atmos. Sci.* **20**, 130 (1963).
- [29] B. S. V. Patnaik and G. W. Wei, *Phys. Rev. Lett.* **88**, 054502 (2002).
- [30] D. C. Wan, B. S.V. Patnaik, and G. W. Wei, *Numer. Heat Transfer, Part B* **40**, 199 (2001).
- [31] G. Hu, J. Yang, and W. Liu, *Phys. Rev. E* **58**, 4440 (1998).
- [32] The engineering aspects of controlling turbulence are described by M. Gad-el-Hak, in *Flow Control: Fundamentals and Practices*, edited by M. Gad-el-Hak, A. Pollard, and J.-P. Bonnet (Springer-Verlag, New York, 1998).
- [33] R. H. Kraichnan and D. Montgomery, *Rep. Prog. Phys.* **43**, 547 (1980); U. Frisch, *Turbulence* (Cambridge University Press, Cambridge, 1995).
- [34] S. Y. Yang, Y. C. Zhou, and G. W. Wei, *Comput. Phys. Commun.* **143**, 113 (2002).
- [35] S. Guan, C.-H. Lai, and G. W. Wei, *Comput. Phys. Commun.* **155**, 77 (2003).
- [36] P. Orlandi, *Fluid Flow Phenomena, A Numerical Toolkit* (Klu-

- wer Academic Publishers, Netherlands, 2000).
- [37] R. Konnur, Phys. Rev. Lett. **77**, 2937 (1996).
- [38] G. S. Duane and J. J. Tribbia, Phys. Rev. Lett. **86**, 4298 (2001).
- [39] M. Inoue, T. Kawazoe, Y. Nishi, and M. Nagadome, Phys. Lett. A **249**, 69 (1998).
- [40] R. Femat and G. Solís-Perales, Phys. Lett. A **262**, 50 (1999).
- [41] C. van Vreeswijk, Phys. Rev. E **54**, 5522 (1996).
- [42] Y. Zhang, G. Hu, H. A. Cerdeira, S. Chen, T. Braun, and Y. Yao, Phys. Rev. E **63**, 026211 (2001).
- [43] Z. Liu, Y.-C. Lai, and F. C. Hoppensteadt, Phys. Rev. E **63**, 055201 (2001).
- [44] N. F. Rulkov, M. M. Sushchik, L. S. Tsimring, and H. D. I. Abarbanel, Phys. Rev. E **51**, 980 (1995).
- [45] H. D. I. Abarbanel, N. F. Rulkov, and M. M. Sushchik, Phys. Rev. E **53**, 4528 (1996).
- [46] G. Chen and S. T. Liu, Chaos, Solitons Fractals **22**, 35 (2004).
- [47] K. Pyragas, Phys. Rev. E **54**, R4508 (1996).
- [48] U. Parlitz, L. Junge, and L. Kocarev, Int. J. Bifurcation Chaos Appl. Sci. Eng. **9**, 2305 (1999).
- [49] J. Sommeria, J. Fluid Mech. **170**, 139 (1986); B. Legras, P. Santangelo, and R. Benzi, Europhys. Lett. **5**, 37 (1988); T. Dubos, A. Babiano, J. Paret, and P. Tabeling, Phys. Rev. E **64**, 036302 (2001).